View metadata, citation and similar papers at core.ac.uk
brought to you by CORE
provided by Elsevier - Publisher Connector

Thin Solid Films 578 (2015) 31–37

Contents lists available at ScienceDirect

Thin Solid Films

journal homepage: www.elsevier.com/locate/tsf

Effect of deposition conditions and post deposition anneal on reactively sputtered titanium nitride thin films

Nikhil K. Ponon *, Daniel J.R. Appleby, Erhan Arac, P.J. King, Srinivas Ganti, Kelvin S.K. Kwa, Anthony O'Neill

School of Electrical and Electronic Engineering, Newcastle University, Newcastle upon Tyne NE1 7RU, United Kingdom

ARTICLE INFO

Article history:
Received 29 May 2014
Received in revised form 17 December 2014
Accepted 3 February 2015
Available online 10 February 2015

Keywords:
Titanium nitride
Reactive sputtering
Resistivity
Annealing
X-ray photoelectron spectroscopy
X-ray diffraction

ABSTRACT

Titanium nitride (TiN_x) was deposited by reactive sputtering using a titanium target in a nitrogen ambient. Nitrogen flow rate during deposition was varied in order to investigate its effect on film resistivity. Conductivity is found to improve with increasing nitrogen content. Films were then annealed, varying the time and temperature of the anneal. Resistivity was found to decrease with longer annealing time and higher temperature during post deposition annealing. TiN_x films showed good thermal and electrical stability upon annealing and did not show any silicon diffusion. It was found that film orientation can influence the resistivity, with [111] oriented films more resistive than [200] oriented films. Moreover, re-crystallization effects brought on by post deposition annealing cause the resistivity to decrease. Films deposited above 20% nitrogen flow rates during deposition were all stoichiometric TiN. However, TiN_x deposited at very high nitrogen flow rate was found to be electrically, thermally and morphologically more stable than the ones deposited at low nitrogen flow rates.

© 2015 The Authors. Published by Elsevier B.V. This is an open access article under the CC BY license (http://creativecommons.org/licenses/by/4.0/).

1. Introduction

Titanium nitride (TiN) is an extremely hard material with high thermal and chemical stability and low electrical and thermal resistivity [1]. It has found many applications in the microelectronics industry as a diffusion barrier [2], gate material [3], Schottky barrier contact [4], adhesion layer [5], and as an electrode in dynamic random access memory cells as well as a back-end-of-line metal–insulator–metal capacitor electrode in integrated circuits [6]. With the increased use of metal nitrides in front-end-of-line processes, which may undergo a post deposition anneal at a temperature well above 500 °C, the stability of these materials at process-relevant temperatures is of paramount interest. The stability of titanium nitride is also key for high temperature electronic circuits as they can be used as capacitor electrodes and transistor gate electrodes in wide-gap semiconductor devices [7].

TiN_x can be deposited in a variety of ways [8–11]. One such method is direct current (DC) magnetron reactive sputtering. This inexpensive technique can deposit films that have high purity and uniformity, with a good control over stoichiometry. In reactive sputtering, the quality of the deposited films depends upon deposition parameters such as nitrogen content in the chamber during deposition, power, residual oxygen in the chamber, pressure, substrate temperature and substrate bias [11]. In the case of integrated circuit applications, TiN_x with better electrical properties may be preferred over stoichiometric TiN.

In microelectronic applications there are constraints on the use of high substrate temperatures during deposition. This is to avoid structural and compositional changes to other materials used in device manufacture and to prevent any uncontrolled diffusion or metal extrusion [12]. However, these structures may undergo a controlled high temperature rapid thermal process (RTP) for dopant activation, dielectric crystallization or metal–semiconductor interface activation. Hence, understanding the impact of post deposition annealing on TiN_x is crucial. To date, there are currently no detailed investigations reported in the literature on the role of post deposition annealing in an oxygen-free ambient above 500 °C on TiN_x deposited with various nitrogen contents. Many research groups have reported that the resistivity of sputtered TiN increases between 100 μΩcm and 1000 μΩcm [13–15] after annealing in a non oxidizing environment in the 500 °C–800 °C range, which is claimed to be due to the oxygen impurity in the annealing ambient [16]. A drastic increase in the sheet resistance after the RTP process would increase the parasitic resistance and resistor–capacitor circuit delays and is not generally desirable from a semiconductor device point of view. Moreover, a sheet resistance value below 400 μΩcm is typically preferred when they are used as the gate electrode of a metal–oxide–semiconductor field effect transistor (MOSFET). [14,17]. Here, we have annealed the samples in high vacuum conditions (1.3×10^{-4} Pa) at temperatures ranging from 500 °C to 900 °C and time varying from 1 min to 20 min in order to avoid the effect of oxygen impurity in the annealing process. The impact of nitrogen flow rate relative to that of argon (N_2 / N_2 + Ar) during deposition, and the post deposition thermal treatment of TiN_x are discussed in this paper. In comparison to other studies, results show that resistivity in fact decreases

* Corresponding author.
E-mail address: nikhil.ponon@ncl.ac.uk (N.K. Ponon).

http://dx.doi.org/10.1016/j.tsf.2015.02.009
0040-6090/© 2015 The Authors. Published by Elsevier B.V. This is an open access article under the CC BY license (http://creativecommons.org/licenses/by/4.0/).

with increase in nitrogen flow rate during deposition, annealing temperature and time. It was found that there is more than one factor which affects the resistivity of the film. Based on these results, reasons for the drop in resistivity with increase in nitrogen flow rate and with a post anneal are assessed in section 3.

1.1. Experimental details

TiN_x was sputtered in an Oxford plasma 400 DC magnetron sputtering system using an eight inch high purity (99.995%) titanium target in a mixture of argon and nitrogen gas. 80 nm thick thermally oxidized silicon dioxide on <100> oriented silicon was used as the substrate. The system was baked out at 100 °C for 12 h which reduced the chamber pressure to 1.3×10^{-4} Pa. Further improvement in the vacuum was achieved by depositing titanium on a dummy wafer in two steps of 15 min each, which reduced the vacuum of the system to 1.3×10^{-5} Pa. The sputtered titanium is believed to react with the remaining oxygen in the chamber creating oxides and thereby reducing the gas pressure inside the chamber.

The deposition time was set to 10 min with the chamber pressure kept at 0.5 Pa. The base pressure was 1.3×10^{-5} Pa and the power used was 800 W for all experiments based on the initial optimization experiments. Step height, measured using atomic force microscopy (AFM), showed that the thickness variation was from 130 nm to 170 nm corresponding with the variation in nitrogen content. The flow rate of nitrogen relative to that of argon was varied from 20% to 95% in order to produce samples of varying stoichiometry. The substrate temperature was limited to 250 °C in order to closely mimic the fabrication condition for both front and back end of line integration. In order to examine the role of high temperature processing on TiN_x thin film properties, as-deposited samples deposited at different nitrogen flow rates were annealed in high vacuum (1.3×10^{-4} Pa). Annealing processes were carried out at 500, 700 and 900 °C for 1, 2, 10 and 20 min.

Sheet resistance was measured at room temperature by a standard four point probe measurement technique. Phase composition and crystallinity were characterized by X-ray diffraction (XRD) with Cu-K_α X-ray radiation having a characteristic wavelength of 1.5418 Å. The powder X-ray diffractometer was set up in the Bragg–Brentano geometry. The X-rays were generated from a Cu anode supplied with 40 kV and a current of 40 mA. Ar ions with beam current 5 mA, an acceleration of 5 kV and a square raster of 1 mm were used to etch the sample for X-ray photoelectron spectroscopy (XPS) depth profiling. The X-ray spot size was 110 μm for the XPS measurements. Raman spectroscopy was used to identify vacancies in the film. A 514 nm laser was used for Raman spectroscopy measurements. The acquisition time was 30 s and the confocal aperture was set to 300 μm. Surface roughness of the deposited film was measured using Park Systems XE 150 AFM in non contact mode. The majority of the material analyses were carried out on samples deposited at lowest nitrogen content (20%) and highest nitrogen content (95%), in order to isolate the physical/structural origins of any observed differences in resistivity.

2. Results

2.1. Variations in resistivity

Changes in resistivity as a function of nitrogen flow rate during TiN_x deposition and for different annealing temperatures for a 1 minute anneal are shown in Fig. 1. The resistivity of the as-deposited samples is also shown and is highest when the nitrogen flow rate is lowest (20%). Resistivity reduces with increasing nitrogen content during TiN_x deposition and reaches the lowest value of 80 μΩcm for the highest nitrogen content of 95%. The resistivity of the films reduces with increasing annealing temperatures for all nitrogen contents, and falls to 35 μΩcm for the sample deposited at 95% nitrogen content when annealed at 900 °C for 1 minute. Resistivity values for different

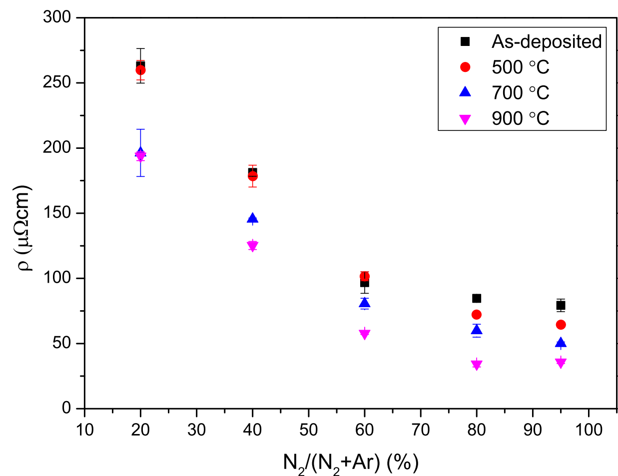

Fig. 1. Variation of TiN_x resistivity with annealing temperature for a fixed annealing time of 1 min. Resistivity decreases with increase in annealing temperature for all nitrogen flow rates.

annealing times at fixed annealing temperatures of 500 °C, 700 °C and 900 °C are shown in Fig. 2. Resistivity drops with annealing time and the lowest value of 30 μΩcm was obtained when annealing the highest nitrogen content sample for 20 min. It can be clearly observed that the resistivity is inversely proportional to nitrogen content during deposition, annealing time and annealing temperature. The highest resistivity was present for the as-deposited samples deposited in 20% nitrogen ambient. The lowest resistivity was obtained when the nitrogen flow was at its highest (95%) and when annealed at 900 °C for 20 min. The variation in the material properties after a post deposition anneal is discussed in the following sections.

2.2. Variations in orientation

The XRD patterns of TiN_x deposited at 20% or 95% nitrogen ambient and then annealed at 700 °C for 1 min and 10 min are shown in Fig. 3. The 20% sample shows a main peak associated with the [111] orientation at around 36.7°, whereas the 95% sample shows a weaker peak for [111] orientation and a predominant peak for [200] orientation around 42.8°. The XRD peak positions confirm that samples deposited at various nitrogen pressures are all TiN phases [18]. The relative intensity (I[111]/I[200]) from the XRD patterns is shown in Fig. 4. TiN_x films with the highest I[111]/I[200] intensity in XRD patterns demonstrate the highest resistivity; these are also the films deposited at lowest nitrogen content. The I[111]/I[200] XRD peak intensity and the resistivity decrease with increasing nitrogen flow rate for the as-deposited samples. These results demonstrate that the resistivity of TiN_x depends on the phase orientation. However, after post deposition annealing, the change in I[111]/I[200] intensity was not proportional to the annealing time even though the resistivity decreased with increasing annealing time. Moreover, the I[111]/I[200] XRD peak intensity increased when compared to that of the as-deposited sample deposited in 60% nitrogen ambient. This would suggest that there is more than one factor directly influencing the resistivity of the film. These other factors affecting the resistivity of the film are investigated in the following sections.

2.3. Variations in vacancies

Raman spectra of the as-deposited and annealed samples (10 min, 700 °C) for 20% and 95% nitrogen flow rate during TiN_x deposition are shown in Fig. 5. Refractory materials such as TiN_x contain both titanium and nitrogen vacancies even for stoichiometric samples. Due to these vacancies, defect induced first-order Raman scattering is possible even though TiN has a symmetric cubic lattice [19]. Raman spectra for TiN_x

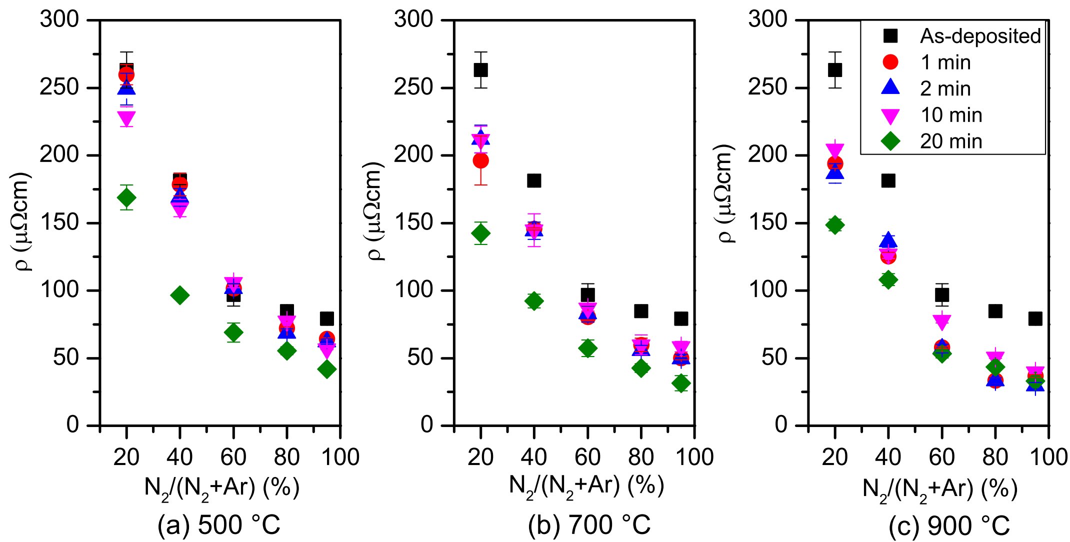

Fig. 2. Variation in TiN_x resistivity with annealing time for a fixed annealing temperature of (a) 500 °C, (b) 700 °C and (c) 900 °C. Resistivity decreases with increase in annealing time for all nitrogen flow rates. The lowest value of resistivity was obtained for the sample deposited at highest nitrogen flow rate (95%) and annealed at highest annealing temperature (900 °C) and longest annealing time (20 min).

show two broad bands in the 150 cm^{-1}–300 cm^{-1} region and one around 550 cm^{-1}. The bands below 300 cm^{-1} (titanium peaks) arise due to acoustic transitions (LA and TA) and the band around 550 cm^{-1} (nitrogen peak) is due to optic modes (LO and TO) [19,20]. Raman scattering in the acoustic range is characterized by vibrations of the relatively heavy titanium ions, and the scattering at the optic range is due to lighter nitrogen ions. The presence of titanium modes indicates nitrogen vacancies, and the existence of nitrogen modes indicates titanium vacancies [21]. The slight variations in the peak positions in Fig. 5 correspond with small variations in vacancy concentrations [22]. The intensity ratio of the titanium to nitrogen peak is a semi-quantitative method to analyze the deviations in vacancy concentrations. The titanium/nitrogen peak intensity ratio is near unity for the as-deposited samples deposited at various nitrogen levels. However, after annealing, the titanium/nitrogen peak intensity decreases considerably for all the samples. An increase in the nitrogen peak intensity would indicate the creation of titanium vacancies. It is possible that the titanium slightly oxidizes due to the presence of residual oxygen in the chamber, creating titanium vacancies in the TiN_x lattice. Nevertheless, the influence on resistivity from oxidation is minimal and, as such, the resistivity in the annealed films does not increase. The increase in oxygen concentration after annealing is confirmed through XPS and is discussed in detail in the next section.

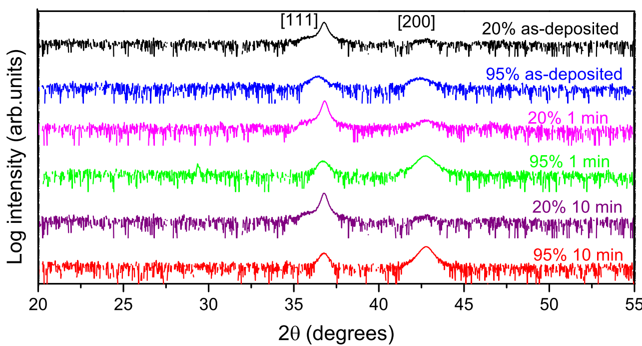

Fig. 3. XRD patterns of TiN_x 20% and 95% samples as-deposited, and annealed at 700 °C for 1 min and 10 min. 20% samples are [111] oriented whereas 95% samples are predominantly [200] oriented.

2.4. Variations in stoichiometry

The variations in stoichiometry were analyzed using XPS spectra. A top layer of TiN_x was etched away in the XPS chamber in order to remove contamination at the surface. High resolution XPS spectra of N *1s*, O *1s* and Ti *2p* as-deposited and annealed samples are shown in Fig. 6. The Ti *2p3/2* for TiN occurs at around 455.0 eV for all nitrogen to argon flow ratios. This is consistent with literature values for stoichiometric TiN [23]. The binding energy for Ti *2p3/2* remains the same after annealing. The variations in binding energy between different nitrogen to argon flow rates and between as-deposited and annealed samples are less than 0.02 eV. This indicates that there is minimal variation in stoichiometry for TiN_x between these samples. The high shoulder regions in Fig. 6(c) for the Ti *2p1/2* and the Ti *2p3/2* peaks correspond with the nitrogen/titanium atom ratio and found to be the highest for stoichiometric TiN [23]. However, the oxide phases and oxynitride phases of titanium also occur at the same binding energy. This means that the presence of small amounts of oxide cannot be confirmed through XPS spectra of titanium as the peaks are masked. Similar to the titanium spectra, N *1s* spectra also do not vary between the samples under

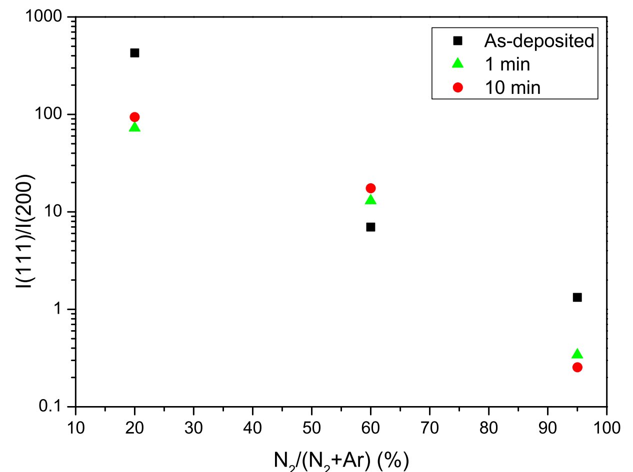

Fig. 4. Relative intensity of [111] peak to [200] peaks in XRD patterns against variation in nitrogen flow rate. Relative intensity decreases with increase in nitrogen flow rate.

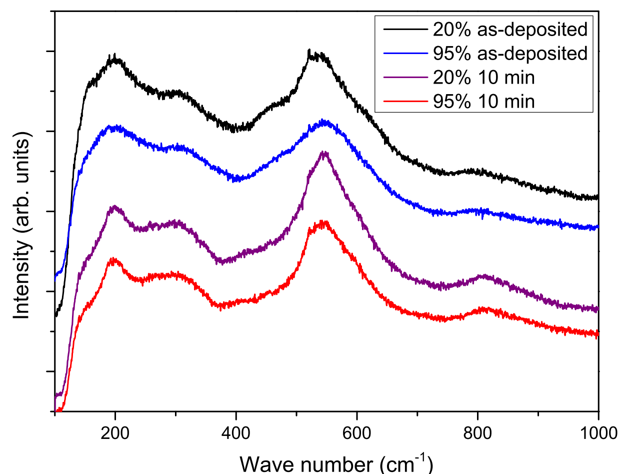

Fig. 5. Raman spectra of as-deposited and annealed (700 °C, 10 min) TiN_x deposited at 20% and 95% nitrogen flow rate.

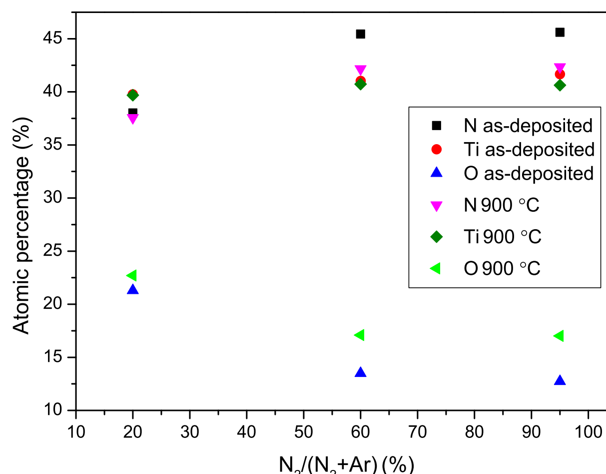

Fig. 7. Variation in nitrogen, oxygen and titanium concentration obtained from XPS spectra for TiN_x deposited at various gas flow rates, before and after anneal.

investigation, again indicating the consistency in stoichiometry before and after annealing for samples deposited at different gas flow rates. The N *1s* spectra of TiN_x are observed at 397.3 eV, consistent with previous studies for stoichiometric TiN [24]. The low intensity, high binding energy peak can be attributed to the oxynitride phases. O *1s* spectra (Fig. 6(b)) are contributed by oxygen atoms from the oxides.

The variations in concentration of nitrogen, oxygen and titanium based on the XPS analysis are given in Fig. 7. The 20% as-deposited sample is nitrogen deficient and the 60% and the 95% as-deposited samples are nitrogen rich. The 20% sample contains greater concentrations of oxygen impurities, compared to the nitrogen rich films which have 13% oxygen impurity concentrations. After post deposition annealing, oxygen levels have increased slightly for all samples. Oxygen may have been introduced from the remaining oxygen in the vacuum chamber which was maintained at a pressure of 1.3×10^{-4} Pa. This oxygen would react with titanium in TiN_x to make oxides. This oxide formation creates titanium vacancies in the lattice, causing an increase in nitrogen mode peak intensity in the Raman spectra as discussed earlier. There is no variation in the titanium concentration after annealing, as expected. The nitrogen content also remains the same for the 20% sample after annealing. The nitrogen content for the nitrogen rich samples (60% and 95%) reduces after the annealing process. This could be due to the release of nitrogen which was precipitated at the grain boundaries [25] while annealing. However, these samples remain slightly nitrogen rich even after annealing at 900 °C for 20 min.

The XPS depth profile of the 95% sample annealed at 700 °C for 10 min is shown in Fig. 8. On the surface, the elemental contributions are different compared to the bulk. The sample surface has a high concentration of carbon and oxygen. This is due to contributions from hydrocarbons and/or surface hydration. After an initial etching cycle, these contaminants reduce. Carbon was not observed in the bulk of the film. The concentration of nitrogen is higher than that of titanium throughout the film, similar to the high resolution spectra results discussed in the earlier section. It is also apparent that there is no diffusion of silicon from the bottom SiO_2 showing good barrier properties. Diffusion of silicon dioxide into TiN_x during annealing at temperatures above 500 °C is a known issue [26]. However, here we have shown that the TiN_x deposited at high nitrogen content prevents the diffusion of SiO_2. Oxygen concentration is almost 15% throughout the film, which might have been introduced by the contamination in the nitrogen source during deposition [27].

2.5. Variations in surface morphology

The variations in the surface roughness as a function of nitrogen to argon flow for the as-deposited sample and one annealed at 900 °C for 20 min are presented in Fig. 9. The root mean square (rms) roughness decreases with increasing nitrogen flow rate. After the anneal, the variation in surface roughness is more than double for lower nitrogen flow rate samples compared to the ones deposited at higher nitrogen content. Surface roughness of TiN_x deposited at high nitrogen flow does not vary greatly after an anneal, showing good stability. Fig. 10 shows the AFM topography scan of as-deposited samples deposited in 20% and 95% nitrogen flow rates. The surface roughness on the 20% sample in Fig. 10(a) is found to be much larger than the 95% sample shown in Fig. 10(b).

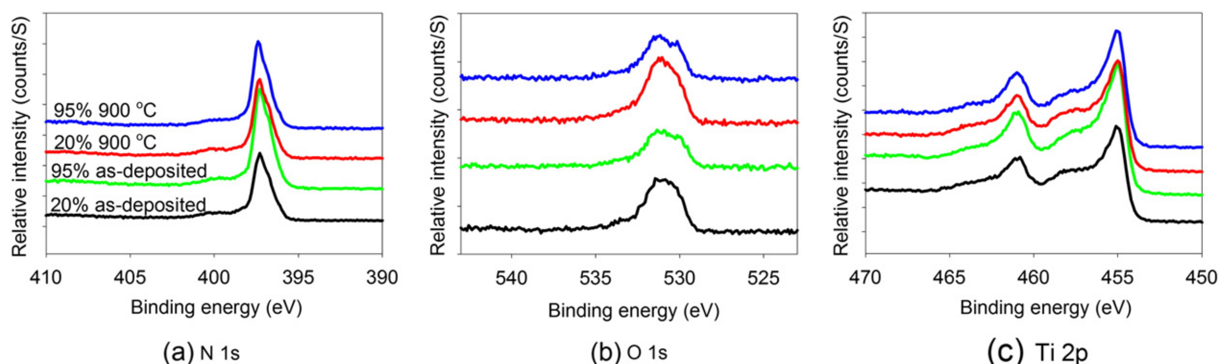

Fig. 6. High resolution XPS spectra of (a) N *1s*, (b) O *1s* and (c) Ti *2p* of as-deposited and annealed (900 °C, 20 min) deposited at 20% and 95% nitrogen content.

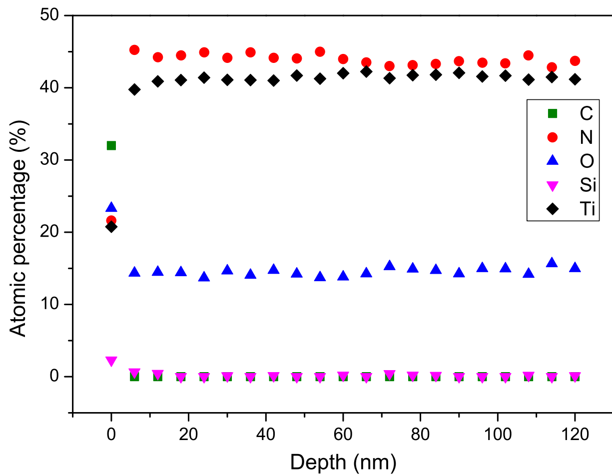

Fig. 8. XPS depth profile of TiN_x deposited at 95% nitrogen and annealed at 700 °C for 10 min. Sample is slightly nitrogen rich. There is no silicon diffusion from the substrate. The oxygen contamination is believed to be from the nitrogen source.

3. Discussion

The resistivity of any thin film is determined mainly by phase, composition, defects (impurities) and microstructure, provided that the measurement temperature remains the same. The XRD peak positions and the XPS binding energy of titanium and nitrogen spectra indicate that the films deposited at various nitrogen flow rates consist of TiN phases and are all stoichiometric. Based on the XPS data shown in Fig. 7, the ratio of titanium concentration to that of nitrogen for 20% samples is 0.96 which increases to 1.04 for 95% samples, after deducting the nitrogen which was believed to be precipitated at grain boundaries for high nitrogen content samples. The variations in stoichiometry are very small, given the large variation in nitrogen partial pressure, which was obtained by varying the flow rate from 20% to 95%. TiN_x deposited above 7% nitrogen flow rate were found to contain stoichiometric TiN phases [28]. However, the variation in nitrogen flow rate and hence the nitrogen partial pressure in the chamber during deposition has a huge impact on the crystalline orientation of the film. Samples deposited at 20% nitrogen flow rate were predominantly [111] oriented compared to the 95% sample which showed a predominant [200] orientation (Fig. 3). We believe that this variation in the orientation is the primary cause for the observed decrease in resistivity with increase in nitrogen flow rate, indicating that [200] orientation is more conductive than [111]. The decrease in resistivity of the as-deposited TiN_x films with decrease in I[111]/I[200] intensity was also observed in previous studies [29,30].

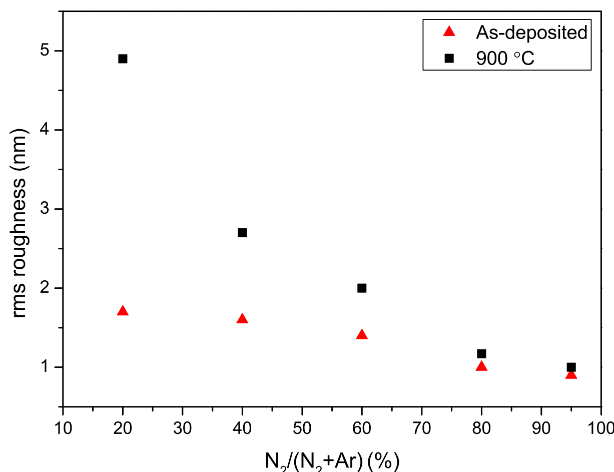

Fig. 9. Surface roughness of as-deposited and annealed (900 °C, 20 min) against various gas flow rates. Surface roughness increases for low nitrogen content samples compared to high nitrogen content samples, indicating good stability against annealing for the high nitrogen content samples.

One of the main causes of resistivity variations in thin films is the scattering of conductive electrons via lattice defects. Raman spectra of as-deposited samples showed that the defect densities are identical with variations in nitrogen flow rates. However, there is a gradual decrease in surface roughness with increase in nitrogen flow rate as shown in Fig. 9. TiN_x with [111] orientation has been found to have a different surface structure compared with the [200] oriented films leading to variations in the surface roughness [30]. We have seen that the [200] phase increases with an increase in nitrogen flow rate during deposition. Therefore, the increase in the [200] phase decreases the surface roughness and increasing nitrogen content contributes towards the increase in conductivity. AFM topography scans shown in Fig. 10 confirm the variation in the surface structure with differences in crystallographic orientation. The sample which showed predominant [200] orientation (95% nitrogen flow) is found to have a much smoother surface than the one with [111] orientation (20% nitrogen flow). A smoother surface helps in the reduction of electron scattering and improves the conductivity. In addition, the resistivity of TiN_x can also depend on film stoichiometry. Since the variation in stoichiometry is negligible, the reason for the decrease in resistivity with nitrogen flow rate for the as-deposited samples is the variation in the crystallographic orientation.

XPS results have confirmed that TiN_x deposited at various nitrogen flow rates are all stoichiometric TiN, although there are differences in the nitrogen concentration of the film. However, the observed decrease in resistivity after annealing cannot be explained by the orientation of the film as the variation in relative intensities after annealing shows a random behavior (Fig. 4). This indicates the possibility of a secondary mechanism which is contributing towards the decrease in resistivity for all samples after annealing. A post-deposition anneal typically results in re-crystallization and crystal growth of the as-deposited amorphous material. All the samples have shown an increase in crystallization after annealing, as it is evident from the XRD patterns (Fig. 3). An increase in grain size would reduce the number of scattered conducting electrons at grain boundaries, in turn reducing the resistivity. An increase in the anneal temperature or duration will increase grain size, leading to a reduction in electron scattering, which can explain the annealing temperature and time dependence on resistivity as shown in this study.

The values for nitrogen content used for TiN_x deposition in the literature are varied, with the majority using nitrogen content lower than 50% [11]. Higher nitrogen content had resulted in diffusion of excess nitrogen to the surface and subsequent desorption, nitrogen precipitation in grain boundaries [25] or superstructure formation [31]. However, here we have shown that higher nitrogen content is in fact beneficial to achieve low resistivity, making the films more suitable for microelectronic applications. Stoichiometrically, films deposited at various nitrogen contents are all TiN. However, these films show variations in electrical, material and morphological properties based on the nitrogen flow rate used during deposition. TiN deposited at high nitrogen content showed least variation in resistivity after annealing, offering better electrical stability compared to the TiN deposited at low nitrogen content. The nitrogen rich films also prevented the diffusion of silicon during annealing, showing good thermal stability. Moreover, the films deposited at higher nitrogen content showed the lowest variation in surface roughness upon annealing, demonstrating better mechanical stability. We have also shown that the slight oxidation of the film during annealing did not affect the resistivity adversely. The reduction in resistivity due to grain growth during annealing superseded the effects due to oxidation or the increase in surface roughness of the film.

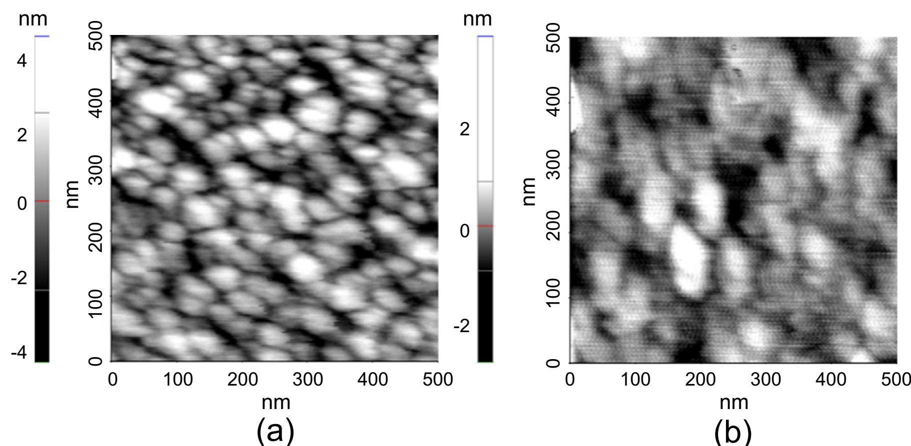

Fig. 10. AFM topography scan of as-deposited film deposited with (a) 20% and (b) 95% nitrogen flow. The surface irregularities on the 20% sample are much larger than the 95% sample.

4. Conclusions

We have investigated the effect of post deposition annealing in an oxygen free environment on the material and electrical properties of reactive sputtered TiN_x. As-deposited TiN_x resistivity showed a gradual decrease with increase in nitrogen flow rate during deposition. The lowest resistivity of 80 μΩcm was obtained for nitrogen rich films. The variations in orientation and therefore the surface roughness are found to be the reason for this decrease in resistivity. TiN_x films sputtered at various nitrogen contents showed good stability and improved stoichiometry after a post deposition RTP in vacuum, without showing any silicon diffusion. Resistivity of these films decreased from the as-deposited levels upon annealing, and went down with annealing time and temperature. The re-crystallization and grain growth led to a further reduction in resistivity. XPS results showed that films deposited at various nitrogen flow rates are all TiN phases. However, films deposited with lower nitrogen content (20%) are titanium rich compared to films deposited with higher nitrogen content which are nitrogen rich. The nitrogen rich films showed least variation in resistivity and morphology. It was also observed that small traces of oxygen do not impact the resistivity of the film. Resistivity of TiN_x is found to reduce after annealing in an oxygen free environment showing a good thermal and electrical stability. This study concludes that, though variation in the nitrogen flow rate and thereby the nitrogen partial pressure during deposition does not have a large influence on the stoichiometry of the film, the nitrogen partial pressure can influence the orientation and the morphology. Films deposited at higher nitrogen partial pressures are electrically, thermally and morphologically more stable than the ones deposited at low nitrogen content. Such films would be more suitable when they are used as diffusion barrier, gate electrode of MOSFETs, adhesion layer or as capacitor electrodes in integrated circuits.

Acknowledgments

This work was funded by the UK Engineering and Physical Sciences Research Council (EPSRC) (EP/H023666/1). Nikhil K. Ponon also acknowledges the PhD studentship support from Intel Corporation Ltd as part of the same grant.

References

[1] J.-E. Sundgren, Structure and properties of TiN coatings, Thin Solid Films 128 (12) (1985) 21.
[2] N. Yokoyama, K. Hinode, Y. Homma, LPCVD titanium nitride for ULSIs, J. Electrochem. Soc. 138 (1) (1991) 190.
[3] M.C. Lemme, J.K. Efavi, T. Mollenhauer, M. Schmidt, H.D.B. Gottlob, T. Wahlbrink, H. Kurz, Nanoscale TiN metal gate technology for CMOS integration, Microelectron. Eng. 83 (2006) 1551.
[4] C.A. Dimitriadis, S. Logothetidis, I. Alexandrou, Schottky barrier contacts of titanium nitride on n-type silicon, Appl. Phys. Lett. 66 (4) (1995) 502.
[5] R. Dauskardt, M. Lane, Q. Ma, N. Krishna, Adhesion and debonding of multi-layer thin film structures, Eng. Fract. Mech. 61 (1) (1998) 141.
[6] M. Lukosius, C. Walczyk, M. Fraschke, D. Wolansky, H. Richter, C. Wenger, High performance metal–insulator–metal capacitors with atomic vapor deposited HfO_2 dielectrics, Thin Solid Films 518 (15) (2010) 4380.
[7] V. Talyansky, R. Vispute, R. Ramesh, R. Sharma, T. Venkatesan, Y. Li, L. Salamanca-Riba, M. Wood, R. Lareau, K. Jones, A. Iliadis, Fabrication and characterization of epitaxial AlN/TiN bilayers on sapphire, Thin Solid Films 323 (1–2) (1998) 37.
[8] J. Westlinder, T. Schram, L. Pantisano, E. Cartier, A. Kerber, G.S. Lujan, J. Olsson, G. Groeseneken, On the thermal stability of atomic layer deposited TiN as gate electrode in MOS devices, IEEE Electron Device Lett. 24 (9) (2003) 550.
[9] N. Mustapha, R. Howson, Optical TiN films by filtered arc evaporation, Surf. Coat. Technol. 92 (1997) 29.
[10] K. Lal, A.K. Meikap, S.K. Chattopadhyay, S.K. Chatterjee, M. Ghosh, K. Baba, R. Hatada, Electrical resistivity of titanium nitride thin films prepared by ion beam-assisted deposition, Phys. B Condens. Matter 307 (14) (2001) 150.
[11] Y.L. Jeyachandran, Sa.K. Narayandass, D. Mangalaraj, Sami Areva, J.A. Mielczarski, Properties of titanium nitride films prepared by direct current magnetron sputtering", Mater. Sci. Eng.: A 445–446 (2007) 223.
[12] P. Roquiny, F. Bodart, G. Terwagne, Colour control of titanium nitride coatings produced by reactive magnetron sputtering at temperature less than 10 °C, Surf. Coat. Technol. 116119 (1999) 278.
[13] K.-C. Park, K.-B. Kim, Effect of annealing of titanium nitride on the diffusion barrier property in Cu metallization, J. Electrochem. Soc. 142 (9) (1995) 3109.
[14] G. Sjoblom, J. Westlinder, J. Olsson, Investigation of the thermal stability of reactively sputter-deposited TiN gate electrodes, IEEE Trans. Electron Devices 52 (10) (2005) 2349.
[15] J.-P. Ao, Y. Naoi, Y. Ohno, Thermally stable TiN Schottky contact on AlGaN/GaN heterostructure, Vacuum 87 (2013) 150.
[16] F.-H. Lu, J.-L. Lo, The influences of oxygen impurity contained in nitrogen gas on the annealing of titanium nitride, J. Eur. Ceram. Soc. 22 (8) (2002) 1367.
[17] H. Park, M. Chang, M. Jo, R. Choi, B.H. Lee, H. Hwang, Device performance and reliability characteristics of tantalum–silicon–nitride electrode/hafnium oxide n-type metal-oxide-semiconductor field-effect transistor depending on composition, Jpn. J. Appl. Phys. 48 (2009) 116506.
[18] F. Vaz, J. Ferreira, E. Ribeiro, L. Rebouta, S. Lanceros-Méndez, J.A. Mendes, E. Alves, Ph. Goudeau, J.P. Rivière, F. Ribeiro, I. Moutinho, K. Pischow, J. de Rijk, Influence of nitrogen content on the structural, mechanical and electrical properties of TiN thin films, Surf. Coat. Technol. 191 (2005) 317.
[19] W. Spengler, R. Kaiser, A.N. Christensen, G. Müller-Vogt, Raman scattering, superconductivity, and phonon density of states of stoichiometric and nonstoichiometric TiN, Phys. Rev. B 17 (1978) 1095.
[20] W. Spengler, R. Kaiser, H. Bilz, Resonant raman scattering in a superconducting transition metal compound TiN, Solid State Commun. 17 (1) (1975) 19.
[21] H.C. Barshilia, K. Rajam, Raman spectroscopy studies on the thermal stability of TiN, CrN, TiAlN coatings and nanolayered TiN/CrN, TiAlN/CrN multilayer coatings, J. Mater. Res. 19 (11) (2004) 3196.
[22] R. Chowdhury, R.D. Vispute, K. Jagannadham, J. Narayan, Characteristics of titanium nitride films grown by pulsed laser deposition, J. Mater. Res. 11 (6) (1996) 1458.
[23] M.J. Vasile, A.B. Emerson, F.A. Baiocchi, The characterization of titanium nitride by X-ray photoelectron spectroscopy and rutherford backscattering, J. Vac. Sci. Technol. A 8 (1) (1990) 99.
[24] C. Nunes Kirchner, K.H. Hallmeier, R. Szargan, T. Raschke, C. Radehaus, G. Wittstock, Evaluation of thin film titanium nitride electrodes for electroanalytical applications, Electroanalysis 19 (10) (2007) 1023.

[25] L. Hultman, J.-E. Sundgren, L.C. Markert, J.E. Greene, Ar and excess N incorporation in epitaxial TiN films grown by reactive bias sputtering in mixed Ar/N_2 and pure N_2 discharges, J. Vac. Sci. Technol. A 7 (3) (1989) 1187.
[26] K.G. Grigorov, G.I. Grigorov, M. Stoyanova, J.L. Vignes, J.P. Langeron, P. Denjean, J. Perriere, Diffusion of Si in titanium nitride films. Efficiency of TiN barrier layers, Appl. Phys. A 55 (1992) 502.
[27] T. Nakano, K. Hoshi, S. Baba, Effect of background gas environment on oxygen incorporation in TiN films deposited using UHV reactive magnetron sputtering, Vacuum 83 (3) (2008) 467.
[28] N.D. Cuong, D.-J. Kim, B.-D. Kang, S.-G. Yoon, Effects of nitrogen concentration on structural and electrical properties of titanium nitride for thin-film resistor applications, Electrochem. Solid-State 9 (9) (2006) G279.
[29] L.-J. Meng, M.D. Santos, Characterization of titanium nitride films prepared by d.c. reactive magnetron sputtering at different nitrogen pressures, Surf. Coat. Technol. 90 (no. 1–2) (1997) 64.
[30] B. Hahn, J. Jun, J. Joo, Plasma conditions for the deposition of tin by biased activated reactive evaporation and dependence of the resistivity on preferred orientation, Thin Solid Films 153 (13) (1987) 115.
[31] S. Zerkout, S. Achour, A. Mosser, N. Tabet, On the existence of superstructure in TiN_x thin films, Thin Solid Films 441 (12) (2003) 135.